

Mean Temperature Profiles in Turbulent Thermal Convection

Olga Shishkina*

Max Planck Institute for Dynamics and Self-Organization, Am Fassberg 17, 37077 Göttingen, Germany

Susanne Horn†

Earth, Planetary, and Space Sciences, University of California, Los Angeles, USA

Mohammad S. Emran‡

Max Planck Institute for Dynamics and Self-Organization, Am Fassberg 17, 37077 Göttingen, Germany

Emily S. C. Ching§

Department of Physics, The Chinese University of Hong Kong, Shatin, Hong Kong

(Dated: October 3, 2018)

To predict the mean temperature profiles in turbulent thermal convection, the thermal boundary layer (BL) equation including the effects of fluctuations has to be solved. In [Shishkina *et al.*, Phys. Rev. Lett. 114 (2015)], the thermal BL equation with the fluctuations taken into account as an eddy thermal diffusivity has been solved for large Prandtl-number fluids for which the eddy thermal diffusivity and the velocity field can be approximated respectively as a cubic and a linear function of the distance from the plate. In the present work we make use of the idea of Prandtl’s mixing length model and relate the eddy thermal diffusivity to the stream function. With this proposed relation, we can solve the thermal BL equation and obtain a closed-form expression for the dimensionless mean temperature profile in terms of two independent parameters for fluids with a general Prandtl number. With a proper choice of the parameters, our predictions of the temperature profiles are in excellent agreement with the results of our direct numerical simulations for a wide range of Prandtl numbers from 0.01 to 2547.9 and Rayleigh numbers from 10^7 to 10^9 .

PACS numbers: 44.20.+b, 44.25.+f, 47.27.ek, 47.27.te

I. INTRODUCTION

Turbulent thermal convection is a major topic in geophysical and astrophysical fluid dynamics and an important problem in engineering and technological applications. The classical systems to study turbulent thermal convection are Rayleigh–Bénard convection (RBC) [1–5] where a fluid is confined between a heated bottom plate and a cooled top plate and horizontal convection (HC) [6–8] in which the fluid is heated at one end of the bottom plate and cooled at the other end of the bottom plate.

One important and well-studied question in turbulent thermal convection research [4, 7, 9, 10] is how the mean convective heat and momentum transport, represented by the Nusselt number (Nu) and Reynolds number (Re) respectively, depend on the main input parameters of the system, which are the Rayleigh number $Ra \equiv \alpha g \Delta H^3 / (\kappa \nu)$ and the Prandtl number $Pr \equiv \nu / \kappa$. Here ν denotes the kinematic viscosity, κ the thermal diffusivity, α the isobaric thermal expansion coefficient of the fluid, g the acceleration due to gravity, H the distance between the heated plate (part) and the cooled plate (part) for RBC (HC), and $\Delta \equiv T_h - T_c > 0$ with

T_h and T_c respectively the temperatures of the heated plate (part) and the cooled plate (part) for RBC (HC). The dependence of Nu and Re on Ra and Pr is influenced significantly by the imposed boundary conditions [11–19]. Grossmann and Lohse developed a scaling theory (GL) [4, 9] for RBC, which nowadays allows one to predict Nu and Re if the pre-factors [10] fitted with the latest experimental and numerical data are used. The GL theory was later extended to the case of HC [7] and magnetoconvection [20].

Closely related to the scaling problem of the heat and momentum transport in different convective systems is the problem to predict the spatial profiles of the mean flow characteristics. Among which, the time- and horizontally area-averaged profile of the temperature as a function of the vertical distance z from the heated bottom plate is of particular research interest. In the Oberbeck–Boussinesq approximation of RBC, the mean temperature depends only weakly on z in the core part of the domain. There exists a certain region in the bulk in which the mean temperature behaves as a logarithmic function of z [21], and this logarithmic region is expected to almost fill the entire bulk for very large Ra [22]. Near to the bottom and top plates, the mean temperature changes much more rapidly with z than in the bulk. The knowledge of these boundary layer (BL) profiles of the mean temperature near the bottom and top plates is important for many engineering applications as well as for the development of reliable turbulence models for thermal

* Olga.Shishkina@ds.mpg.de

† SusanneHorn@ucla.edu

‡ Mohammad.Emran@ds.mpg.de

§ ching@phy.cuhk.edu.hk

convection. It remains one of the most challenging unsolved problems to predict the mean temperature boundary layer profiles.

In its derivation of the heat and momentum transport scalings in BL-dominated regimes in RBC, the GL theory [4, 9] assumes that the viscous BL thickness is proportional to $\text{Re}^{-1/2}$. This scaling relation holds, in particular, in the classical Prandtl-Blasius (PB) boundary-layer theory [23, 24] for steady flows. The mean temperature profiles obtained in experimental and numerical studies have been compared against the profiles obtained from the PB theory, and systematic deviations were reported [25–30]. The deviations are generally larger for larger Ra and smaller Pr and they remain even after an application of a dynamical rescaling procedure [31] that takes into account the time variation of the BL thickness.

In the PB theory, the pressure gradient vanishes and fluctuations do not exist. The effect of a non-zero pressure gradient within the BLs, or equivalently the effect of a large-scale mean circulating flow that is not parallel to the isothermal plate, was studied in Shishkina *et al.* [32] and led to the BL equations, which are similar to those of Falkner and Skan (FS) [33]. With the FS approach one calculates the ratio of the thermal to viscous BL thicknesses more accurately compared to PB but the FS approximation does not lead to a significantly better prediction of the mean temperature profiles, as the limits of the PB and FS profiles for infinitesimal Pr are the same [34]. For large Pr and a flow with a constant shear rate, Shraiman and Siggia [35] derived the mean temperature profile and the relation between the heat flux and shear rate in thermal convection. Their mean temperature profile also coincides with the PB prediction for infinitely large Pr [25]. Ching [36] generalized their approach to the case of a position-dependent shear rate and derived the temperature profile as a function of two parameters which are associated with the local thermal BL thickness and the shear rate. Good agreement of these derived profiles with the actual ones can be obtained only when the two parameters are taken as free fitting parameters.

In Shishkina *et al.* [37] we derived a new thermal BL equation for turbulent RBC in large-Pr fluids. The equation takes into account the effect of fluctuations, which are neglected in the PB or FS BL equations, using an eddy thermal diffusivity. In the case of large Pr, the thermal BL is nested within the viscous BL, thus the eddy thermal diffusivity and the horizontal mean velocity can be approximated respectively as a cubic and a linear function of the distance from the plate. For the limits $\text{Pr} \gtrsim 1$ and $\text{Pr} \rightarrow \infty$ of such simplification of the BL equations for large Pr, the mean temperature profiles were analytically obtained and shown to be in very good agreement with the profiles obtained in Direct Numerical Simulations (DNS) of RBC for, respectively, $\text{Pr} = 4.38$ (water) and $\text{Pr} = 2547.9$ (glycerol).

In the present paper we shall derive a thermal BL equation for fluids with a general Pr, including very small

Pr. We extend the approximation of the eddy thermal diffusivity to larger z and propose an approximate relation between the eddy thermal diffusivity and the stream function within the thermal BL. Then we can solve the resulting thermal BL equation to obtain the mean temperature profiles in terms of two independent parameters. With a proper choice of the parameters, our theoretical predictions are in perfect agreement with the mean temperature profiles obtained in the DNS for Pr down to 0.01. Our present approach can be reduced to that of [37] in the case of large Pr.

II. BASIC EQUATION

Following [37], we consider the quasi two-dimensional fluid flow along a semi-infinite horizontal heated plate and assume that far away from the plate, there exists a constant mean velocity, the wind, along a horizontal x -direction x . The equation for the temperature field $T(x, z, t)$ is

$$\partial_t T + \mathbf{u} \cdot \nabla T = \kappa \nabla^2 T, \quad (1)$$

where $\mathbf{u}(x, z, t) \equiv u(x, z, t) \hat{x} + v(x, z, t) \hat{z}$ is the velocity field, and the flow is incompressible:

$$\nabla \cdot \mathbf{u} = 0. \quad (2)$$

Using Reynolds decomposition of the flow fields into sums of time-averages and fluctuations,

$$u = U + u', \quad v = V + v', \quad T = \Theta + \theta', \quad (3)$$

in (1) and averaging it in time afterwards, we obtain the following equation for the time-averaged temperature:

$$U \partial_x \Theta + V \partial_z \Theta + \partial_x \langle u' \theta' \rangle_t + \partial_z \langle v' \theta' \rangle_t = \kappa \partial_z^2 \Theta + \kappa \partial_x^2 \Theta, \quad (4)$$

where $\langle \cdot \rangle_t$ denotes the time-averaging. The continuity equation (2) holds for both the mean and fluctuating velocities:

$$\partial_x U + \partial_z V = 0, \quad (5)$$

$$\partial_x u' + \partial_z v' = 0. \quad (6)$$

As usual for BLs, we assume that within the BL $|\partial_x^2 \Theta| \ll |\partial_z^2 \Theta|$ and $|\partial_x \langle u' \theta' \rangle_t| \ll |\partial_z \langle v' \theta' \rangle_t|$ and obtain

$$U \partial_x \Theta + V \partial_z \Theta + \partial_z \langle v' \theta' \rangle_t = \kappa \partial_z^2 \Theta. \quad (7)$$

Introducing the eddy thermal diffusivity $\kappa_t(x, z)$ for the fluctuation term in (7), which is defined by

$$\langle v' \theta' \rangle_t \equiv -\kappa_t \partial_z \Theta, \quad (8)$$

we obtain

$$U \partial_x \Theta + (V - \partial_z \kappa_t) \partial_z \Theta = (\kappa + \kappa_t) \partial_z^2 \Theta. \quad (9)$$

In the BL in turbulent thermal convection the eddy thermal diffusivity is not negligible [37]. To satisfy (5) we introduce the stream function Ψ , such that

$$U = \partial_z \Psi, \quad V = -\partial_x \Psi. \quad (10)$$

We define the similarity variable ξ and the dimensionless stream function $\psi(\xi)$ and temperature $\theta(\xi)$:

$$\xi \equiv z/\lambda(x), \quad (11)$$

$$\Psi \equiv U_0 \lambda(x) \psi(\xi), \quad (12)$$

$$\Theta \equiv T_h - (\Delta/2)\theta(\xi). \quad (13)$$

and look for a similarity solution of (9) in terms of ξ . Here $\lambda(x)$ is the local thickness of the thermal BL, U_0 is the maximal horizontal velocity (wind velocity), T_h is the temperature of the heated bottom plate, and $\Delta/2$ is the temperature difference between the bottom plate and the bulk of the flow. Substituting (11)–(13) into (9), we obtain the following dimensionless thermal BL equation:

$$(1 + \kappa_t/\kappa)\theta_{\xi\xi} + [(\kappa_t/\kappa)_{\xi} + B\psi]\theta_{\xi} = 0 \quad (14)$$

with

$$B = U_0 \lambda \lambda_x / \kappa. \quad (15)$$

The subscripts ξ and x denote the ordinary derivative with respect to ξ and x . For a similarity solution to exist, κ_t/κ should depend on ξ only and B must be a constant, independent of x , therefore $\lambda(x) \propto \sqrt{x}$. With

$$\lambda(x) \propto \sqrt{\nu x / U_0}, \quad (16)$$

from (15) we obtain that $B \propto \text{Pr}$. It follows from (16) that the viscous BL thickness scales as $\text{Re}^{-1/2}$, where $\text{Re} \equiv U_0 x / \nu$, if the ratio of thicknesses of the viscous and thermal BLs depends only on Pr .

To solve the thermal BL equation (14) with the boundary conditions

$$\theta(0) = 0, \quad \theta_{\xi}(0) = 1, \quad \theta(\infty) = 1, \quad (17)$$

and obtain the dimensionless temperature profiles $\theta(\xi)$, we need to know $\kappa_t(\xi)/\kappa$ and $\psi(\xi)$. In the next two sections we will establish an approximation of $\kappa_t(\xi)$ and propose an approximate relation between $\kappa_t(\xi)$ and $\psi(\xi)$.

III. EDDY THERMAL DIFFUSIVITY

Very close to the plate, the eddy thermal diffusivity can be approximated as a cubic function of ξ [37]. In this regard, the eddy thermal diffusivity and the eddy viscosity exhibit similar behavior near the plate [38]. From the continuity equation (6) of the fluctuating velocity it follows that $\partial_z v' = 0$ at the plate ($z = 0$). From this result and the fact that all fluctuations u' , v' and θ' vanish at $z = 0$, we obtain consequentially

$$\langle v'\theta' \rangle_t|_{z=0} = 0, \quad \partial_z \langle v'\theta' \rangle_t|_{z=0} = 0, \quad \partial_z^2 \langle v'\theta' \rangle_t|_{z=0} = 0. \quad (18)$$

Using the definition of κ_t (8) and the linear dependency of ξ on z [see (11)], these results imply

$$\kappa_t|_{\xi=0} = (\kappa_t)_{\xi}|_{\xi=0} = (\kappa_t)_{\xi\xi}|_{\xi=0} = 0 \quad (19)$$

and, hence, close to the plate, κ_t/κ can be approximated as a cubic function of ξ ,

$$\kappa_t/\kappa \approx a^3 \xi^3, \quad (20)$$

with a certain constant a , which measures the size of fluctuations.

Relatively far away from the plate, the mean temperature Θ behaves as a logarithmic function of the distance z from the plate [22, 39, 40]. In this logarithmic or inner region, the fluctuations are so strong that the term $\partial_z \langle v'\theta' \rangle_t$ dominates the other terms on the left-hand side of (7),

$$\partial_z \langle v'\theta' \rangle_t \approx \kappa \partial_z^2 \Theta, \quad (21)$$

which implies

$$\langle v'\theta' \rangle_t \approx \kappa [\partial_z \Theta - \partial_z \Theta|_{z=0}] \approx -\kappa \partial_z \Theta|_{z=0} \quad (22)$$

as in the inner region the mean temperature Θ changes very slowly with z so that $|\partial_z \Theta|_z \ll |\partial_z \Theta|_{z=0}$. Using (8) and (22), we have

$$(\kappa_t/\kappa) \partial_z \Theta \approx \partial_z \Theta|_{z=0} \quad (23)$$

The logarithmic dependence on z of Θ thus implies that κ_t/κ behaves as a linear function of z or ξ in this region:

$$\kappa_t/\kappa \sim \xi. \quad (24)$$

These two different behaviors of κ_t/κ on ξ , (20) for small ξ and (24) for large ξ , have both been demonstrated in [37].

Based on these two behaviors, we make the following approximation of $(\kappa_t/\kappa)_{\xi}$:

$$(\kappa_t/\kappa)_{\xi} \approx \frac{3a^3 \xi^2}{1 + b^2 \xi^2}, \quad (25)$$

where b is a constant that determines the location ξ_{\max} of the maximum value of $(\kappa_t/\kappa)_{\xi\xi}$, namely

$$\xi_{\max} = (\sqrt{3}b)^{-1}. \quad (26)$$

From (25) we obtain

$$\frac{\kappa_t}{\kappa} \approx \frac{3a^3}{b^3} [b\xi - \arctan(b\xi)]. \quad (27)$$

which gives the two limiting behaviors discussed above, namely

$$\frac{\kappa_t}{\kappa} \approx 3a^3 \left(\frac{\xi^3}{3} + \frac{b^2 \xi^5}{5} + \frac{b^4 \xi^7}{7} + \mathcal{O}(\xi^9) \right) \approx a^3 \xi^3 \quad (28)$$

for $\xi \rightarrow 0$, and

$$\frac{\kappa_t}{\kappa} \approx 3a^3 \left(\frac{\xi}{b^2} - \frac{\pi}{2b^3} + \frac{1}{b^4 \xi} + \mathcal{O}(\xi^{-3}) \right) \approx \frac{a^3}{b^2} \xi \quad (29)$$

for $\xi \rightarrow \infty$.

IV. PROPOSED RELATION BASED ON MIXING LENGTH MODEL

We first make use of the idea of Prandtl's mixing length model [41] to relate κ_t to the mean velocity gradient. According to Prandtl's mixing length model, a fluid parcel will retain its velocity for a mixing length l_v before mixing with surrounding fluid in a turbulent environment. Thus, the fluctuation in the velocity can be seen as the difference in velocity between a distance l_v . As all fluctuations in the thermal BL are mostly along the vertical z -direction, we use this picture to approximate the vertical velocity fluctuation v' by

$$v' \approx l_v \partial_z V. \quad (30)$$

Similarly, we approximate the temperature fluctuation θ' by

$$\theta' \approx -l_\theta \partial_z \Theta, \quad (31)$$

where l_θ is the mixing length for temperature. Using (30) and (31), we have

$$\langle v' \theta' \rangle_t \approx -l_v l_\theta \partial_z V \partial_z \Theta. \quad (32)$$

Comparing (32) with (8), we obtain

$$\kappa_t / \kappa \approx (l_v l_\theta / \kappa) \partial_z V, \quad (33)$$

which relates the eddy thermal diffusivity to the mean velocity gradient.

Next, we evaluate (33) near the plate to get a direct relation between $(\kappa_t / \kappa)_\xi$ and ψ . Near the plate, we estimate the mixing lengths to be proportional to z :

$$l_v \approx k_v z, \quad l_\theta \approx k_\theta z, \quad (34)$$

where k_v and k_θ are some positive constants. Substituting (34) into (33) and using (10)-(12) and (15), we thus have

$$\kappa_t / \kappa \approx B k_v k_\theta \xi^3 \psi_{\xi\xi} \quad (35)$$

Taking the derivative of (35) w.r.t. ξ and keeping only the lowest order term in ξ , we obtain

$$(\kappa_t / \kappa)_\xi \approx 3B k_v k_\theta \xi^2 \psi_{\xi\xi}(0) \quad \text{for small } \xi. \quad (36)$$

On the other hand, using $\psi(0) = \psi_\xi(0) = 0$ that result from the no-slip boundary condition, we obtain

$$\psi \approx \psi_{\xi\xi}(0) \xi^2 / 2 \quad \text{for small } \xi. \quad (37)$$

Hence, (36) and (37) give

$$(\kappa_t / \kappa)_\xi \approx 6B k_v k_\theta \psi \quad \text{for small } \xi, \quad (38)$$

establishing a similarity between the dimensionless stream function ψ and the derivative of the eddy thermal diffusivity $(\kappa_t / \kappa)_\xi$ near the plate.

The mean horizontal velocity U grows linearly with distance close to the plate. At a certain distance from the plate it attains a maximum value (which gives the wind velocity) and then decays to zero towards the bulk of the flow. From (10) and (12), $U = U_0 \psi_\xi$, and ξ is linearly related with the vertical coordinate z , therefore, the dimensionless stream function ψ goes as ξ^2 near the plate and is almost constant far away from the plate. Thus, the functional dependences of ψ and $(\kappa_t / \kappa)_\xi$ on ξ are similar in two limits: both of them $\sim \xi^2$ for $\xi \rightarrow 0$ and $\sim \text{const}$ for $\xi \rightarrow \infty$. This observation together with (38) motivate us to propose the following approximate relation for the whole thermal BL:

$$(\kappa_t / \kappa)_\xi \approx KB \psi \quad (39)$$

for some constant $K > 0$.

V. THEORETICAL MODEL

Using the proposed relation (39), we obtain

$$(\kappa_t / \kappa)_\xi + B \psi \approx (1 + 1/K)(\kappa_t / \kappa)_\xi \equiv c(\kappa_t / \kappa)_\xi, \quad (40)$$

and (14) becomes

$$(1 + \kappa_t / \kappa) \theta_{\xi\xi} + c(\kappa_t / \kappa)_\xi \theta_\xi = 0. \quad (41)$$

Equation (41) is a thermal BL equation for all values of Pr , including $\text{Pr} < 1$. When the fluctuations are relatively weak so that the flow remains in the transition from laminar to turbulent state, the value of c can be large. When the fluctuations are so strong that the term $(\kappa_t / \kappa)_\xi$ dominates $B \psi$ in (40), the constant c is close to 1. The solution of (41) is

$$\theta(\xi) = \int_0^\xi \left[1 + \frac{\kappa_t}{\kappa}(\eta) \right]^{-c} d\eta, \quad (42)$$

which together with the approximation (27) yields

$$\theta(\xi) = \frac{1}{b} \int_0^{b\xi} \left[1 + \frac{3a^3}{b^3} (\eta - \arctan(\eta)) \right]^{-c} d\eta. \quad (43)$$

Note that (43) has two independent parameters only as the following must be fulfilled,

$$b = \int_0^\infty \left[1 + \frac{3a^3}{b^3} (\eta - \arctan(\eta)) \right]^{-c} d\eta, \quad (44)$$

due to the boundary conditions far away from the plate, $\theta(\infty) = 1$.

For the particular case of very large Pr , the thermal BL is deeply nested within the viscous BL and the eddy thermal diffusivity can be approximated by (28). Thus, (42) is reduced to the form reported in [37]:

$$\theta(\xi) = \int_0^\xi (1 + a^3 \eta^3)^{-c} d\eta, \quad (45)$$

where the constants a and c are related with

$$a = \frac{\Gamma(1/3)\Gamma(c-1/3)}{3\Gamma(c)} \quad (46)$$

and Γ is the gamma function. As discussed in [37], analytical expressions for θ can be obtained from (45) for $c = 1$, which corresponds to the limiting case of large fluctuations:

$$\theta = \frac{\sqrt{3}}{4\pi} \log \frac{(1+e\xi)^3}{1+(e\xi)^3} + \frac{3}{2\pi} \arctan \frac{2e\xi-1}{\sqrt{3}} + \frac{1}{4} \quad (47)$$

with $e = 2\pi/(3\sqrt{3}) \approx 1.2$ as well as for $c = 2$:

$$\theta = \frac{\sqrt{3}}{4\pi} \log \frac{(1+f\xi)^3}{1+(f\xi)^3} + \frac{3}{2\pi} \arctan \frac{2f\xi-1}{\sqrt{3}} + \frac{\xi}{3(1+(f\xi)^3)} + \frac{1}{4} \quad (48)$$

with $f = 4\pi/(9\sqrt{3}) \approx 0.8$.

Equations (47) and (48) are found to be in good agreement with DNS results for $\text{Pr} = 4.38$ and $\text{Pr} = 2547.9$ respectively, as reported in [37]. For intermediate values of Pr between 4.38 and 2547.9, (45) with a fitted value of c is shown to be in good agreement with DNS results [42].

VI. VALIDATION OF THE MODEL

In [37, 42] we have shown that (45) describes the temperature profiles obtained in DNS of RBC very well in the large- Pr regime, from $\text{Pr} = 4.38$ to $\text{Pr} = 2547.9$. The DNS simulations were conducted in a cylindrical container with a diameter-to-height aspect ratio 1, using the finite-volume computational code GOLDFISH [43]. This code features a high flexibility in the choice of the size of the computational grids, which are finer near the domain boundaries and resolve the Kolmogorov and Batchelor microscales [44]. Our present work aims for a prediction of the temperature profiles for general Pr , and in particular for small Pr . For this purpose, additional simulations for $\text{Pr} = 0.01$, $\text{Pr} = 0.0232$, $\text{Pr} = 0.1$ and $\text{Pr} = 1$ have been performed. Here we will check the new results (43), (44) mostly against these additional DNS data of small Pr , and consider only two cases of large Pr (see Table I for the details of the cases studied). We will also show that for large Pr the new profiles (43) with (44) are very close to our earlier result (45) reported in [37].

We first check directly the validity of (33) with l_v and l_θ given by the approximation (34), which form the basis of our proposed relation (39). As shown in Fig. 1, (33), with l_v and l_θ given by (34) with $k_v k_\theta \approx 1$ indeed holds well near the plates up to $\xi \approx 1$.

Then we check our new results (43), (44) against the DNS data. We normalize the mean temperature profiles θ , obtained in the DNS and averaged in time and over horizontal cross sections, in such a way that θ is equal to 0 at the plate and to 1 in the central part of the domain and its derivative with respect to ξ in the vertical direction is

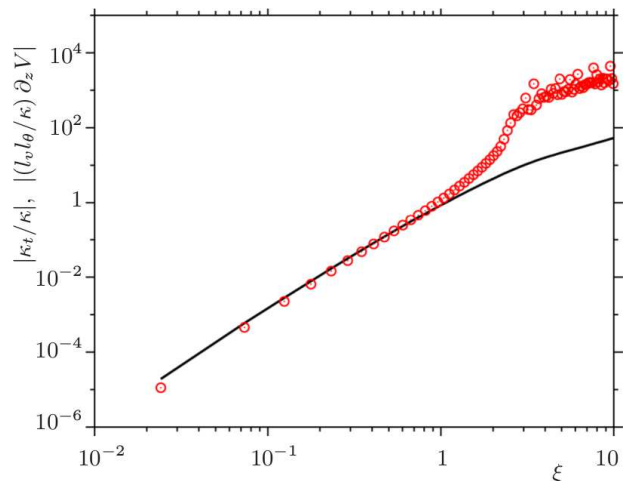


FIG. 1. Normalized eddy thermal diffusivity $|\kappa_t/\kappa|$, calculated for $\kappa_t = (V\Theta - \langle vT \rangle_t) / \partial_z \Theta$, and then averaged over horizontal cross-sections, obtained in the DNS for $\text{Pr} = 10$ and $\text{Ra} = 10^8$ (symbols) together with a fit for $|(l_v l_\theta / \kappa) \partial_z V|$ averaged over horizontal cross-sections (solid line). Here l_v and l_θ are taken according to (34), i.e. $l_v l_\theta \sim z^2$. Thus, the symbols and the line represent, respectively, the magnitudes of the left- and right-hand sides of the assumption (33).

equal to 1 at the plate. For a fixed Pr and varying Ra , the profiles are generally different, see Fig. 2. In laminar and transitional regimes, the mixing in the core part of the domain is limited and different complicated global flow structures develop, which for smaller Ra in some cases may even cause overshoot profiles. With increasing Ra , the temperature profiles start to converge. Thus, in turbulent regime, starting at a certain sufficiently large Ra , all temperature profiles almost coincide. In Fig. 2 one can see that for $\text{Pr} = 0.1$ the temperature profiles differ significantly for Ra from 10^5 to 10^6 and almost replicate each other for $\text{Ra} \geq 5 \times 10^6$. All of them lie outside the region of the Prandtl–Blasius (or Falkner–Skan) predictions for all possible Pr , which is shown in gray colour in Fig. 2. For smaller Ra , the profiles are closer to the PB predictions but the converged temperature profiles clearly lie far outside of the PB region.

We focus now on the temperature profiles of the fully developed turbulent convective flows, i.e. on the converged profiles for sufficiently large Ra . As discussed, these profiles depend strongly on Pr with little or no dependence on Ra . In Fig. 3 such profiles are presented for $\text{Pr} = 0.1$, $\text{Pr} = 1$ and $\text{Pr} = 2547.9$, as obtained in the DNS (symbols) together with the model solutions of (43) (lines of the corresponding colours) for proper choices of the parameters a , b and c . More precisely, the parameter a is found by fitting the DNS data for κ_t/κ by the approximation (28) near the heated plate within half the thermal BL thickness, i.e. for ξ ranging from 0 to 0.5. Then the parameters b and c are sought by fitting (43) to the DNS temperature profiles, while varying c and keeping b satisfying the equation (44). The fitted values of a ,

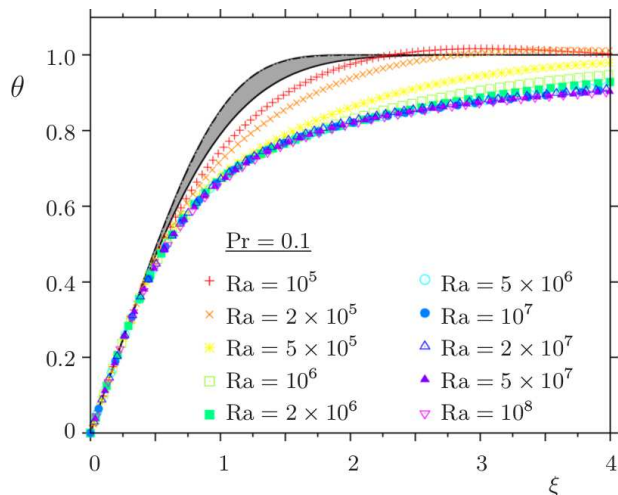


FIG. 2. Temperature profiles, averaged in time and over horizontal cross sections, obtained in the DNS of RBC in a cylindrical container of the aspect ratio 1 for $Pr = 0.1$ and different Ra (symbols). One can see that the profiles converge with increasing Ra . Prandtl–Blasius predictions for $Pr \rightarrow \infty$ (—) and $Pr \rightarrow 0$ (---) bound the gray region of Prandtl–Blasius predictions for all intermediate Pr .

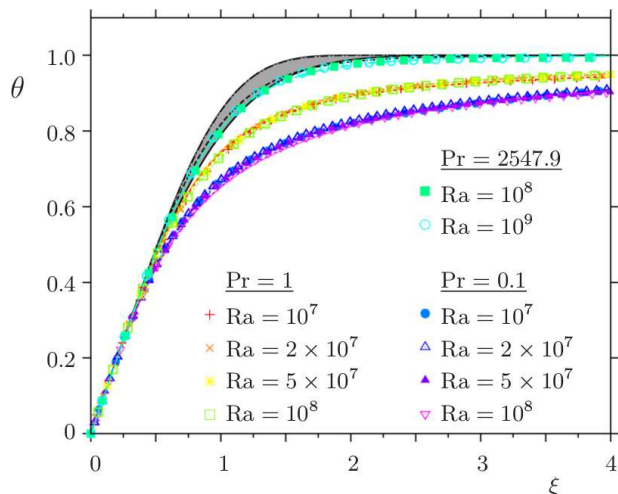


FIG. 3. Temperature profiles, averaged in time and over horizontal cross sections, obtained in the DNS of RBC in a cylindrical container of the aspect ratio 1 for $Pr = 0.1$, $Pr = 1$ and $Pr = 2547.9$ and different Ra (symbols) together with the predictions (43) (lines of the corresponding colours), see Table I. The black dashed line corresponds to the simplification (48) for very large Pr , as reported in [37]. The Prandtl–Blasius region (gray) is as in Fig. 2.

b and c obtained for different Ra and Pr are presented in Table I. Evidently, (43) perfectly describes the temperature profiles in a wide range of Pr including $Pr \ll 1$.

Finally, we consider transitional RBC flows with very small Pr , specifically $Pr = 0.01$ and $Pr = 0.0232$ for $Ra = 10^7$. Also for these RBC flows, the temperature profiles are in excellent agreement with (43), as illus-

Pr	Ra	a	b	c
0.01	10^7	1.59	6.19	4.99
0.0232	10^7	1.56	3.59	2.64
0.1	10^7	1.52	2.27	1.84
0.1	2×10^7	1.49	2.21	1.86
0.1	5×10^7	1.59	2.72	1.97
0.1	10^8	1.62	2.79	1.96
1	10^7	1.16	0.62	1.36
1	2×10^7	1.13	0.63	1.41
1	5×10^7	1.12	0.81	1.57
1	10^8	1.15	0.64	1.39
4.38	10^8	1.00	0.61	1.68
4.38	10^9	1.02	0.62	1.64
2547.9	10^8	0.77	0.51	2.61
2547.9	10^9	0.75	0.52	2.77

TABLE I. Fitted values of the parameters in the temperature profiles approximation (43).

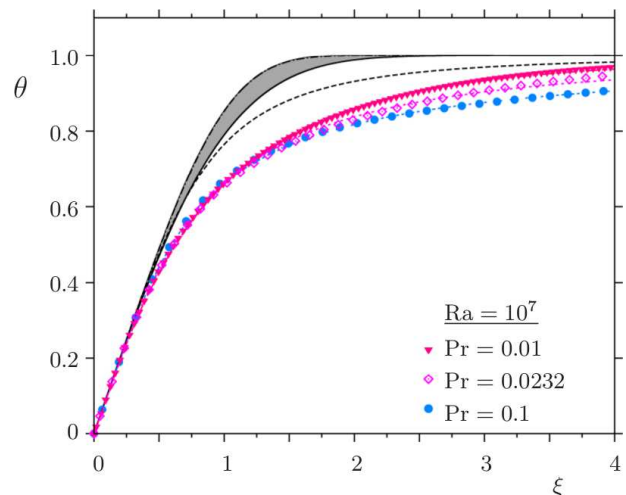


FIG. 4. Temperature profiles, averaged in time and over horizontal cross sections, obtained in the DNS of RBC in a cylindrical container of the aspect ratio 1 for $Ra = 10^7$ and different small Prandtl numbers (symbols) together with the predictions (43) from the present work (lines of the corresponding colours), see Table I. The black dashed line corresponds to the limiting case (47) for the simplification (45) for large Pr . The Prandtl–Blasius region (gray) is as in Fig. 2.

trated in Fig. 4. The corresponding parameters are given in Table I.

VII. CONCLUSIONS

Utilizing the idea of Prandtl’s mixing length model, we put forward an approximate relation between the eddy thermal diffusivity κ_t and the stream function ψ within the thermal BL. This proposed relation has allowed us to obtain a thermal BL equation (41) that takes fluctuations for fluids with a general Pr into account, thus extending our earlier work [37]. Using the present approximation

(27) for the eddy thermal diffusivity for the entire thermal BL, we have obtained the solution (43) of the thermal BL equation (41) in terms of two independent parameters a and c . The third parameter, b , is fixed by the boundary condition far away from the plate, which is given by (44). The parameter a measures the intensity of the fluctuations very close to the plate according to (28) while the parameter $c \geq 1$ reflects the relative magnitudes of the stream function and the derivative of the eddy thermal diffusivity. When the BL flow is highly fluctuating so that the term $(\kappa_t/\kappa)_\xi$ dominates the term $B\psi$ in (40), c is about 1. On the other hand, in a transitional flow with relatively weak fluctuations, the value of c is large. With a proper choice of a and c , our theoretical model (43) describes extremely precisely the temperature profiles near the heated or cooled horizontal plates, in transitional and turbulent convective flows, for very large as well as very small Pr. In the present work, we have obtained the fitted value of a by using DNS data of κ_t/κ near the heated plate. In situations where measurements of κ_t are not available, as in most experimental studies, we suggest to fit the measured temperature profiles directly by (43) with the constraint (44) to get the values of the two independent parameters a and c . Note that our earlier model (45), (46) for the temperature profiles in large-Prandtl-number RBC, which was proposed in [37], has only one free parameter, while the new model (43), (44) has two free parameters but is applicable to general Pr.

To derive empirical formulas for the parameters a and c in the model (43), (44), further experimental and numer-

ical data are needed, in particular for very high Ra and very small Pr. It should be noted that the DNS of RBC by large Ra and either very large Pr [37] or very small Pr [45, 46] require enormous computational efforts due to the requirement to resolve all relevant spatial and temporal microscales [44]. That is, the time stepping must be finer than the time microscale $\tau = (\nu/\epsilon_u)^{1/2}$ and the spatial stepping must be smaller than the Kolmogorov microscale $\eta = (\nu^3/\epsilon_u)^{1/4}$ if $\text{Pr} \leq 1$ or smaller than the Batchelor microscale $\eta_B = (\nu\kappa^2/\epsilon_u)^{1/4}$ if $\text{Pr} > 1$. Here ϵ_u is the mean kinetic dissipation rate, which in RBC equals $\epsilon_u = (\nu^3/H^4)(\text{Nu} - 1)\text{Ra}^2\text{Pr}^{-2}$. For large Pr the need to resolve the time microscale is restrictive, while for small Pr the very fine meshes in space are needed to resolve the Kolmogorov spatial microscale. The general dependence of the temperature profiles (43) on Pr, Ra and the geometrical characteristics of the convection cell will therefore be explored in future when more experimental and numerical data, in particular for very small Pr, will be available.

ACKNOWLEDGMENTS

OS, ME and SH acknowledge the financial support of the Deutsche Forschungsgemeinschaft (DFG) under grants Sh405/4-2 (Heisenberg fellowship), Sh405/3-2 and Ho 5890/1-1. The authors thank the Leibniz Supercomputing Centre (LRZ) for providing computing time.

-
- [1] G. Ahlers, S. Grossmann, and D. Lohse, “Heat transfer and large scale dynamics in turbulent Rayleigh–Bénard convection,” *Rev. Mod. Phys.* **81**, 503–537 (2009).
 - [2] E. Bodenschatz, W. Pesch, and G. Ahlers, “Recent developments in Rayleigh–Bénard convection,” *Annu. Rev. Fluid Mech.* **32**, 709–778 (2000).
 - [3] F. Chillà and J. Schumacher, “New perspectives in turbulent Rayleigh–Bénard convection,” *Eur. Phys. J. E* **35**, 58 (2012).
 - [4] S. Grossmann and D. Lohse, “Scaling in thermal convection: A unifying theory,” *J. Fluid Mech.* **407**, 27–56 (2000).
 - [5] E. S. C. Ching, *Statistics and scaling in turbulent Rayleigh–Bénard convection* (Springer, Singapore, 2014).
 - [6] G. O. Hughes and R. W. Griffiths, “Horizontal convection,” *Ann. Rev. Fluid Mech.* **40**, 185–208 (2008).
 - [7] O. Shishkina, S. Grossmann, and D. Lohse, “Heat and momentum transport scalings in horizontal convection,” *Geophys. Res. Lett.* **43**, 1219–1225 (2016).
 - [8] O. Shishkina and S. Wagner, “Prandtl-number dependence of heat transport in laminar horizontal convection,” *Phys. Rev. Lett.* **116**, 024302 (2016).
 - [9] S. Grossmann and D. Lohse, “Thermal convection for large Prandtl numbers,” *Phys. Rev. Lett.* **86**, 3316–3319 (2001).
 - [10] R. J. A. M. Stevens, E. P. van der Poel, S. Grossmann, and D. Lohse, “The unifying theory of scaling in thermal convection: The updated prefactors,” *J. Fluid Mech.* **730**, 295–308 (2013).
 - [11] S. Grossmann and D. Lohse, “Multiple scaling in the ultimate regime of thermal convection,” *Phys. Fluids* **23**, 045108 (2011).
 - [12] P. Hassanzadeh, G. P. Chini, and C. R. Doering, “Wall to wall optimal transport,” *J. Fluid Mech.* **751**, 627–662 (2014).
 - [13] M. Gibert, H. Pabiou, F. Chillà, and B. Castaing, “High-rayleigh-number convection in a vertical channel,” *Phys. Rev. Lett.* **96**, 084501 (2006).
 - [14] Z. A. Daya and R. E. Ecke, “Does turbulent convection feel the shape of the container?” *Phys. Rev. Lett.* **87**, 184501 (2001).
 - [15] X. He, E. S. C. Ching, and P. Tong, “Locally averaged thermal dissipation rate in turbulent thermal convection: A decomposition into contributions from different temperature gradient components,” *Phys. Fluids* **23**, 025106 (2011).
 - [16] G. Boffetta and R. E. Ecke, “Two-dimensional turbulence,” *Ann. Rev. Fluid Mech.* **44**, 427–451 (2012).
 - [17] C. R. Doering, F. Otto, and M. G. Reznikoff, “Bounds on vertical heat transport for infinite-Prandtl-number Rayleigh–Bénard convection,” *J. Fluid Mech.* **560**, 229–242 (2006).

- [18] O. Shishkina and S. Horn, “Thermal convection in inclined cylindrical containers,” *J. Fluid Mech.* **790**, R3 (2016).
- [19] O. Shishkina, “Momentum and heat transport scalings in laminar vertical convection,” *Phys. Rev. E* **93**, 051102(R) (2016).
- [20] T. Zürner, W. Liu, D. Krasnov, and J. Schumacher, “Heat and momentum transfer for magnetoconvection in a vertical external magnetic field,” *Phys. Rev. E* **94**, 043108 (2016).
- [21] G. Ahlers, E. Bodenschatz, and X. He, “Logarithmic temperature profiles of turbulent Rayleigh–Bénard convection in the classical and ultimate state for a Prandtl number of 0.8,” *J. Fluid Mech.* **758**, 436–467 (2014).
- [22] S. Grossmann and D. Lohse, “Logarithmic temperature profiles in the ultimate regime of thermal convection,” *Phys. Fluids* **24**, 125103 (2012).
- [23] L. Prandtl, “Über Flüssigkeitsbewegung bei sehr kleiner Reibung,” in *Verhandlungen des III. Int. Math. Kongr., Heidelberg, 1904* (Teubner, 1905) pp. 484–491.
- [24] L. D. Landau and E. M. Lifshitz, *Fluid Mechanics*, 2nd ed., Course of Theoretical Physics, Vol. 6 (Butterworth Heinemann, 1987).
- [25] O. Shishkina and A. Thess, “Mean temperature profiles in turbulent Rayleigh–Bénard convection of water,” *J. Fluid Mech.* **663**, 449–460 (2009).
- [26] N. Shi, M. S. Emran, and J. Schumacher, “Boundary layer structure in turbulent Rayleigh–Bénard convection,” *J. Fluid Mech.* **706**, 5–33 (2012).
- [27] J. D. Scheel, E. Kim, and K. R. White, “Thermal and viscous boundary layers in turbulent Rayleigh–Bénard convection,” *J. Fluid Mech.* **711**, 281–305 (2012).
- [28] R. J. A. M. Stevens, Q. Zhou, S. Grossmann, R. Verzicco, K.-Q. Xia, and D. Lohse, “Thermal boundary layer profiles in turbulent Rayleigh–Bénard convection in a cylindrical sample,” *Phys. Rev. E* **85**, 027301 (2012).
- [29] M. Kaczorowski, O. Shishkina, A. Shishkin, C. Wagner, and K.-Q. Xia, “Analysis of the large-scale circulation and the boundary layers in turbulent Rayleigh–Bénard convection,” in *Direct and Large-Eddy Simulation VIII*, edited by H. Kuerten, B. Geurts, V. Armenio, and J. Fröhlich (Springer, 2011) pp. 383–388.
- [30] M. Ovsyannikov, D. Krasnov, M. S. Emran, and J. Schumacher, “Combined effects of prescribed pressure gradient and buoyancy in boundary layer of turbulent Rayleigh–Bénard convection,” *Eur. J. Mech. (B/Fluids)* **57**, 64–74 (2016).
- [31] Q. Zhou and K.-Q. Xia, “Measured instantaneous viscous boundary layer in turbulent Rayleigh–Bénard convection,” *Phys. Rev. Lett.* **104**, 104301 (2010).
- [32] O. Shishkina, S. Horn, and S. Wagner, “Falkner-Skan boundary layer approximation in Rayleigh–Bénard convection,” *J. Fluid Mech.* **730**, 442–463 (2013).
- [33] V. M. Falkner and S. W. Skan, “Some approximate solutions of the boundary layer equations,” *Phil. Mag.* **12**, 865–896 (1931).
- [34] O. Shishkina, S. Wagner, and S. Horn, “Influence of the angle between the wind and the isothermal surfaces on the boundary layer structures in turbulent thermal convection,” *Phys. Rev. E* **89**, 033014 (2014).
- [35] B. I. Shraiman and E. D. Siggia, “Heat transport in high-Rayleigh-number convection,” *Phys. Rev. A* **42**, 3650–3653 (1990).
- [36] E. S. C. Ching, “Heat flux and shear rate in turbulent convection,” *Phys. Rev. E* **55**, 1189–1192 (1997).
- [37] O. Shishkina, S. Horn, S. Wagner, and E. S. C. Ching, “Thermal boundary layer equation for turbulent Rayleigh–Bénard convection,” *Phys. Rev. Lett.* **114**, 114302 (2015).
- [38] R. A. Antonia and J. Kim, “Turbulent Prandtl number in the near-wall region of a turbulent channel flow,” *Int. J. Heat Mass Transfer* **34**, 1905–1908 (1991).
- [39] G. Ahlers, E. Bodenschatz, D. Funfschilling, S. Grossmann, X. He, D. Lohse, R.J.A.M. Stevens, and R. Verzicco, “Logarithmic temperature profiles in turbulent Rayleigh–Bénard convection,” *Phys. Rev. Lett.* **109**, 114501 (2012).
- [40] G. Ahlers, E. Bodenschatz, and X. He, “Logarithmic temperature profiles of turbulent Rayleigh–Bénard convection in the classical and ultimate state for a prandtl number of 0.8,” *J. Fluid Mech.* **758**, 436–467 (2014).
- [41] L. Prandtl, “Bericht über Untersuchungen zur ausgebildeten Turbulenz,” *Z. Angew. Math. Mech.* **5**, 136–139 (1925).
- [42] E. S. C. Ching, O.-Y. Dung, and O. Shishkina, “Fluctuating thermal boundary layers and heat transfer in turbulent Rayleigh–Bénard convection,” *J. Stat. Phys.* **167**, 626–635 (2017).
- [43] G. L. Kooij, M. A. Botchev, E. M.A. Frederix, B. J. Geurts, S. Horn, D. Lohse, E. P. van der Poel, O. Shishkina, R. J. A. M. Stevens, and R. Verzicco, “Comparison of computational codes for direct numerical simulations of turbulent Rayleigh–Bénard convection,” *Comp. Fluids*, submitted (2017).
- [44] O. Shishkina, R. J. A. M. Stevens, S. Grossmann, and D. Lohse, “Boundary layer structure in turbulent thermal convection and its consequences for the required numerical resolution,” *New J. Phys.* **12**, 075022 (2010).
- [45] J. D. Scheel and J. Schumacher, “Global and local statistics in turbulent convection at low Prandtl numbers,” *J. Fluid Mech.* **802**, 147–173 (2016).
- [46] J. Schumacher, V. Bandaru, A. Pandey, and J. D. Scheel, “Transitional boundary layers in low-Prandtl-number convection,” *Phys. Rev. Fluids* **1**, 084402 (2016).